*Research supported by the Army Research Office-Durham, Durham, N. C.

[1]F. C. Witteborn and W. M. Fairbank, Phys. Rev. Letters 19, 1049 (1967).
[2]L. I. Schiff and M. V. Barnhill, Phys. Rev. 151, 1067 (1966).
[3]A. J. Dessler, F. C. Michael, H. E. Rorschach, and G. T. Trammell, Phys. Rev. 168, 737 (1968).
[4]C. Herring, Phys. Rev. 171, 1361 (1968).
[5]G. Papinui, Nuovo Cimento 63B, 549 (1969).
[6]W. A. Harrison, Phys. Rev. 180, 1606 (1969).
[7]L. I. Schiff, Phys. Rev. B 1, 4649 (1970).
[8]P. P. Craig, Phys. Rev. Letters 22, 700 (1969).
[9]G. T. Trammell and H. E. Rorschach, Phys. Rev. B 2, 4761 (1970).
[10]J. W. Beams, Phys. Rev. Letters 21, 1093 (1968).
[11]P. P. Craig and V. Radeka, Rev. Sci. Instr. 41, 258 (1970).
[12]S. H. French and J. W. Beams, Phys. Rev. B 1, 3300 (1970).
[13]M. Cohen, Y. Goldstein, and B. Abeles, Phys. Rev. B 3, 2223 (1971).
[14]C. R. Brown, J. B. Browne, E. Enga, and M. R. Halse, J. Phys. D 4, 298 (1971).
[15]T. J. Rieger, Phys. Rev. B 2, 825 (1970).
[16]W. E. Gordy, Phys. Rev. 69, 604 (1946).
[17]E. P. Gyftopoulos and D. Steiner, Report on the Twenty Seventh Annual Conference on Physical Electronics, Cambridge, Mass., 1967, p. 160 (unpublished).
[18]L. Pauling, *The Nature of the Chemical Bond*, 3rd ed. (Cornell U. P., Ithaca, N. Y., 1960), p. 393.
[19]C. Kittle, *Introduction to Solid State Physics*, 3rd ed. (Wiley, New York, 1968), p. 122.
[20]J. C. Slater, *Quantum Theory of Molecules and Solids* (McGraw-Hill, New York, 1965), Vol. 2, p. 103.
[21]J. C. Schumacher, W. E. Spicer, and W. A. Tiller, Bull. Am. Phys. Soc. 17, 134 (1972).

PHYSICAL REVIEW B VOLUME 6, NUMBER 8 15 OCTOBER 1972

Low-Energy-Electron-Diffraction Rotation Diagrams for the (100) Face of Aluminum*

G. E. Laramore
Sandia Laboratories, Albuquerque, New Mexico 87115
(Received 14 March 1972)

Low-energy-electron-diffraction rotation diagrams are calculated for Al (100), and the results are compared with experimental measurements. The agreement between theory and experiment is qualitatively correct for an energy $E = 50$ eV and an angle of incidence $\theta = 32°$ but is much less satisfactory for $E = 20$ eV and $\theta = 50°$. The effect of small changes in the upper-layer spacing on the calculated rotation diagrams is also investigated. It is found that the primary effect is to change the magnitude of the rotation diagram and not its qualitative shape. This apparent insensitivity to geometrical effects may be an asset in using the rotation diagrams to study resonance effects.

I. INTRODUCTION

Rotation diagrams (intensity vs azimuthal angle for fixed energy and polar angle) provide a unique test of the dynamical characteristics of model calculations of low-energy-electron-diffraction (LEED) intensities. Unlike LEED energy profiles (intensity vs energy for fixed polar and azimuthal angles) where interference effects between kinematic scattering events can produce major features,[1] in the absence of surface imperfections all structure in the rotation diagrams is due to either multiple-scattering effects or resonance effects.[2-5] Recently there have been several experimental measurements and theoretical analyses of LEED rotation diagrams for Al(100) which emphasize the usefulness of the rotation diagrams for studying the effects of the surface potential barrier.[6-8] A possible complicating feature in analyzing the experimental measurements would be undue sensitivity to small uncertainties in the surface geometrical parameters. In the present paper we show that this is not the case by investigating the effect of small changes in the upper-layer spacing on the calculated rotation diagrams. The changes that are produced are more in the nature of an overall normalization change. This is in contrast to the large qualitative changes produced in the calculated LEED energy profiles by small changes in the surface geometrical parameters.[9]

The model used in the present work is the same as used previously by Laramore and Duke[9,10] to analyze experimental energy profiles for the (100), (110), and (111) faces of aluminum. The model allows for refraction, but not reflection, of the electron wave field at the surface; and thus, includes resonances associated with the threshold conditions for the emergence of new beams but not those resonances associated with scattering into surface states. The effect of the surface-state resonances would be to produce local "maxima-minima structures" of the Breit-Wigner form in both the energy profiles[3-5] and rotation diagrams.[6-8] It is interesting to note that the model

calculations, although they do not include the effects of surface-state resonances, produce a broad local maximum-minimum structure near a place where an experimental maximum-minimum structure attributed to a surface-state resonance occurs. However, the details of the predicted structure are in rather poor agreement with the experimental observations.

The experimental rotation diagrams were measured for relatively large angles of incidence measured relative to the surface normal—one set of data is at $E = 20$ eV and $\theta = 50°$ and the other set of data is at $E = 50$ eV and $\theta = 32°$. In previous analyses[9,10] of Jona's experimental LEED intensity profiles[11] from Al(100), we noted that although there was fairly good correspondence between theory and experiment for small angles of incidence, this correspondence deteriorated noticeably at larger angles of incidence. The effect was quite noticeable at $\theta = 20°$. This problem could be due both to the effect of surface morphology, which presumably would become more important at large angles of incidence, and also to the extremely simplified model used to describe the electron-solid interaction as the electron enters and leaves the solid. Nevertheless, the theoretical calculations do an adequate job of reproducing the qualitative features of the experimental rotation diagrams. We also show that small changes in electron energy produce large changes in the calculated rotation diagrams. Such small changes simulate uncertainties in the value of the inner potential used in the calculation and in the experimental measurement of the electron's energy.

In Sec. II we briefly discuss the theoretical model used in the calculations. In Sec. III we apply the model to calculate rotation diagrams for the (00), $(\bar{1}\bar{1})$, $(\bar{1}1)$, $(\bar{2}0)$, and $(\bar{2}\bar{2})$ beams for $E = 50$ eV and $\theta = 32°$ and for the (00), $(\bar{1}1)$, and $(\bar{2}0)$ beams[12] for $E = 20$ eV and $\theta = 50°$. We also show the effect of small changes in the electron energy and in the surface geometrical parameters on the calculated rotation diagrams. Finally, in Sec. IV we summarize our results.

II. DISCUSSION OF MODEL

The basic model used in the calculation has been extensively described elsewhere,[9,10] and so here we simply mention some features relevant to the discussion of the theoretical results. Perhaps the most gross oversimplification of the calculation is the model used to describe the electronic self-energy which we take as[9,10,13]

$$\Sigma(E) = -V_0 - i\Gamma(E), \tag{1}$$

where

$$\Gamma(E) = \frac{\hbar^2}{m\lambda_{ee}} \left(\frac{2m}{\hbar^2}(E + V_0)\right)^{1/2}. \tag{2}$$

In Eqs. (1) and (2), E is the energy of the electron outside the crystal, λ_{ee} is twice the inelastic collision mean free path, and V_0 is the inner potential which we take[9,10] as 16.7 eV. In keeping with previous work, we take $\lambda_{ee} = 8$ Å. For $E = 20$ eV this gives $\Gamma(E) \simeq 3.0$ eV and for $E = 50$ eV this gives $\Gamma(E) \simeq 4.0$ eV. These values for the imaginary part of the electronic self-energy are substantially larger than the values for $\Gamma(E)$ used in the pseudopotential calculations of Refs. 7 and 8, where for $E = 20$ eV a value of $\Gamma(E) = 1.5$ eV was used[8] and for $E = 50$ eV a value of $\Gamma(E) = 1.0$ eV was used.[7] If anything, the experimental measurements by Quinto *et al.*[14] of the energy-dependent effective Debye temperatures for the primary Bragg peaks in the LEED energy profiles from Al(100) indicate even larger values[15] for $\Gamma(E)$ than we use here.

To describe the electron–ion-core scattering we use the $l = 0$, 1, and 2 phase shifts obtained from Snow's augumented-plane-wave (APW) band-structure potential.[16] Plots of these phase shifts are shown in Refs. 9 and 10. We use the rigid-lattice form for the electron–ion-core elastic scattering amplitude, i.e.,

$$t(\vec{k}_2, \vec{k}_1) = \frac{i\pi\hbar^2}{mk} \sum_l (2l+1)(e^{2i\delta_l(k)} - 1)P_l(\cos\theta_{12}), \tag{3}$$

where $k = |\vec{k}_1| = |\vec{k}_2|$, θ_{12} is the angle between $\vec{k}_1$ and $\vec{k}_2$, and the $P_l(\cos\theta_{12})$ are the standard Legendre polynomials. The renormalization effects of the lattice vibrations[17,18] are not included since it is not possible to accurately model the vibronically renormalized electron–ion-core elastic scattering amplitude for the surface ion cores of aluminum (because of their relatively large vibrational amplitude) using only three partial wave components[15] (the computer code available to us at the present time can handle only three partial wave components). Assuming that the experimental rotation diagrams were measured at room temperature ($T \simeq 300$ °K), then it would be possible to do a reasonably accurate job of modeling the vibronically renormalized scattering amplitude for the bulk ion cores ($\Theta_D^B \simeq 380$ °K $> T$), but in this limit the results differ very little from the rigid-ion approximation.

We use reflectivity boundary conditions in the calculation,[9] and so compute an absolute reflectivity. Unfortunately, the units of the experimental measurements are arbitrary.

III. RESULTS

In this section we present a comparison between experimental LEED rotation diagrams[6–8] and the

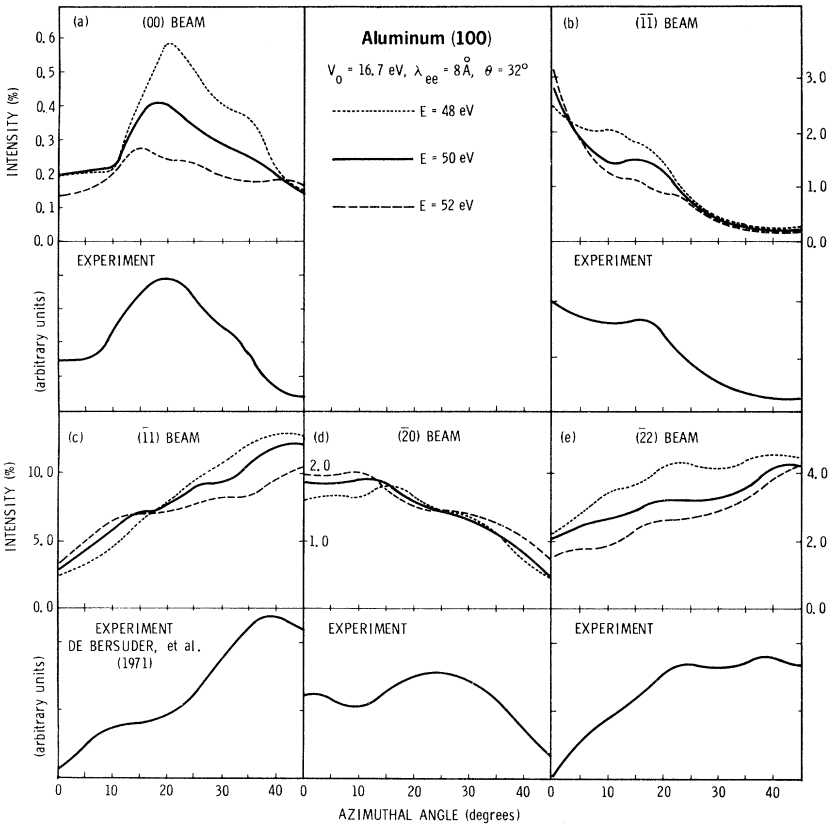

FIG. 1. Comparison between theoretical and experimental (Ref. 7) LEED rotation diagrams for Al (100) for an incident angle of 32°. The theoretical curves are shown for $E = 48$ (dotted curve), 50 (solid durve), and 52 eV (dashed curve); and the experimental curves are shown for $E = 50$ eV. The units of the theoretical curves are in percent reflectivity while the units of the experimental curves are arbitrary. The parameters used in the calculation are shown in the figure. The beams are indexed according to the nonprimitive cubic two-dimensional unit cell.

theoretical curves calculated using the model outlined in Sec. II and also investigate the effect of small changes in the upper-layer spacing of the solid on the calculated rotation diagrams. Curves are shown for both specular and nonspecular beams. We follow the nomenclature of Refs. 6–8 and label the beams according to the nonprimitive cubic two-dimensional unit cell. A diagram explicitly showing the labeling of the beams according to this convention is given by Jona.[11] The azimuthal angle ϕ is measured clockwise with respect to the positive x axis. Because of the symmetry of the (100) face of a cubic material, the rotation diagram is completely specified for $0° \leq \phi \leq 45°$.

In Fig. 1 we show a comparison between the experimental[7] and theoretical rotation diagrams for $E = 50$ eV and $\theta = 32°$. To see the effect of small changes in the assumed value of the inner potential or small errors in measuring the electron energy, theoretical rotation diagrams are also shown for $E = 48$ eV and for $E = 52$ eV. For example, if the actual value of the inner potential were 14.7 eV instead of 16.7 eV, then the dotted theoretical curves would correspond to the experimental curves. We also note that the experimental spread in electron energy[7] is typically of order 1 eV, and so the experimental curves represent an average over some range of energies. This should be kept in mind especially since the theoretical curves exhibit a pronounced dependence on electron energy. The claimed experimental angular resolution[6–8] is 0.1°, and so the angular uncertainty should be negligible. The theoretical curves are measured in percent reflectivity, while the units of the experimental curves are arbitrary. The agreement between theory and experiment is quite good for the (00) and the ($\bar{1}\bar{1}$) beams and is certainly at least qualitatively correct for the other beams as well. This seems especially remarkable when one considers that all departures of the curves from some constant value are due to dynamical effects. Also, no attempt was made to adjust the parameters of the calculation to bring theory and experiment into better correspondence; and the work of de Bersuder *et al.*[7] shows some dependence of the calculated rotation diagrams on $\Gamma(E)$. Although the units of the experimental curves are arbitrary, de Bersuder *et al.*[7] give a figure which shows the relative intensities of the various beams. The calculated intensities of the beams are in good accord with the measured intensities in that the relative over-all strengths of the various beams are ordered correctly. The agreement between theory and experiment (shown in Fig. 1) is substantially better than that obtained in Ref. 7. We next turn to an even more stringent test of the model by con-

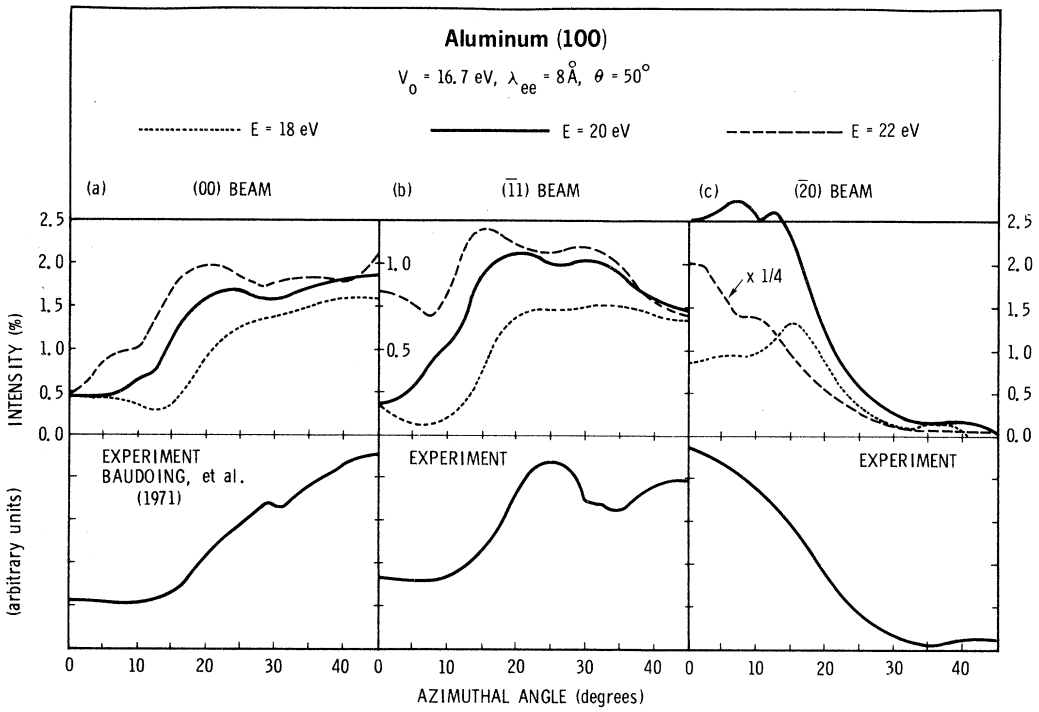

FIG. 2. Comparison between theoretical and experimental (Refs. 6 and 8) LEED rotation diagrams for Al (100) for an incident angle of 50°. The theoretical curves are shown for $E = 18$ eV (dotted curve), 20 eV (solid curve), and 22 eV (dashed curve); and the experimental curves are shown for $E = 20$ eV. The units of the theoretical curves are in percent reflectivity, while the units of the experimental curves are arbitrary. The parameters used in the calculation are shown in the figure. The beams are indexed according to the nonprimitive cubic two-dimensional unit cell.

sidering rotation diagrams of a much lower energy and a much larger angle of incidence. It is here that resonance effects are likely to be important.

In Fig. 2 we show a comparison between the experimental[6,8] and the theoretical rotation diagrams for $E = 20$ eV and $\theta = 50°$. To see the effect of small changes in the assumed value of the inner potential or small errors in measuring the electron energy, theoretical rotation diagrams are also shown for $E = 18$ and 22 eV. The theoretical curves are measured in percent reflectivity, while the units of the experimental curves are arbitrary. The agreement between theory and experiment is substantially poorer than that shown in Fig. 1. This might have been expected since deviations from the model used for the electronic self-energy would show up first for low electron energies at large angles of incidence. There are several things that should be noted about Fig. 2. First note the local maximum-minimum structure in the experimental curve for the specular beam near $\phi \simeq 30°$. This has been attributed to a surface resonance since it does not coincide with the emergence of any new beams.[6,8] Such surface-state resonances are not in our theoretical model. However, the theoretical model does produce a very broad maximum-minimum structure with the position of the minimum coinciding with the experimental minimum; note that this structure is emphasized somewhat by a small expansion of the upper-layer spacing (see Fig. 3). The relatively sharp structure observed experimentally is not produced by the model calculations. The basic trend of the intensity remaining relatively constant until $\phi \simeq 13°$ and then increasing with increasing ϕ is evident in the theoretical curves. Recently, Taub[19] has used a modified version of the isotropic scatterer inelastic collision model to investigate the effects of the surface potential barrier on the energy profiles and rotation diagrams. He finds that the inclusion of a potential barrier can produce a resonance structure in the (00) beam for $E = 20$ eV and $\theta = 40°$ and 50°; but the position and width of the predicted structure disagree with the details of the experimental observations. The pseudopotential calculation of Baudoing *et al.*[8] also gives a resonancelike structure; but it too does not quantitatively agree with the experimental work. For the (20̄) beam, we note that the qualitative feature of the intensity being large at small ϕ and then decreasing as ϕ increases is reproduced in the theoretical curves. However, the theoretical curves exhibit structure between 5° and 13° that is not seen experimentally. This structure looks much like the surface-state-resonance structure

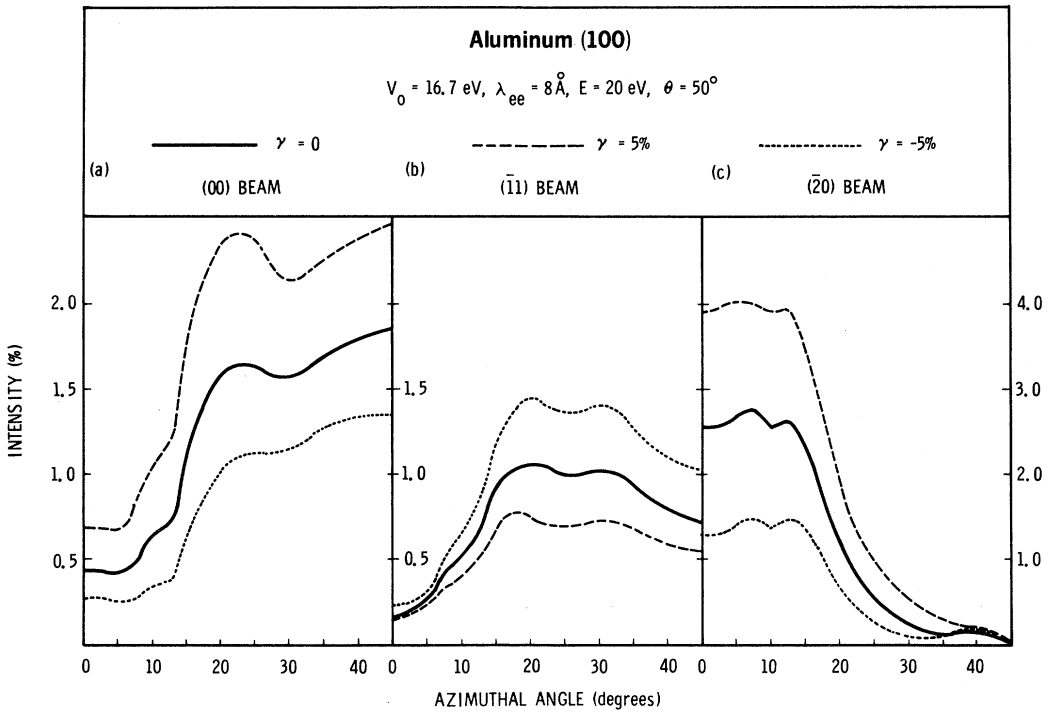

FIG. 3. Effect of small changes in the upper-layer spacing on the calculated rotation diagrams for $E = 20$ eV and $\theta = 50°$. Rotation diagrams are shown for the case where the upper-layer spacing equals the bulk-layer spacing (solid curve), for the case where the upper-layer spacing is contracted by 5% relative to the bulk-layer spacing (dotted curve), and for the case where the upper-layer spacing is expanded by 5% relative to the bulk-layer spacing (dashed curve). The units of the curves are in percent reflectivity; and the beams are indexed according to the nonprimitive cubic two-dimensional unit cell. The parameters used in the calculation are shown in the figure.

seen experimentally for the (00) beam. The $(\bar{1}1)$ beam exhibits the worst agreement of all between theory and experiment. We also note that small energy changes make quite pronounced changes in the calculated profiles and so part of the discrepancy between theory and experiment could be attributed to uncertainty in the value of the inner potential used in the calculation and also due to the experimental spread in electron energies. However, the agreement between theory and experiment is substantially better than for calculations using the s-wave version of the inelastic collision model that are shown in Ref. 8. This shows the importance of the higher partial wave components.

In Fig. 3 we show the effect of small changes in the upper-layer spacing on the calculated rotation diagrams. The spacing between the top two layers in written

$$d' = (1+\gamma)d \ , \tag{4}$$

where γ is the fractional change in the layer spacing, and d is the bulk-layer spacing. Rotation diagrams are shown for $\gamma = 0, \pm 5\%$. Note that although changes of this order give rise to substantial qualitative changes in the LEED energy profiles,[9] this is not the case for the rotation diagrams. Although there are some changes in the details of the fine structure of the rotation diagrams, the main change seems to be simply in the *magnitude* of the beam intensities. Since the model calculations do not give the details of the fine structure correctly, and since it is an exceedingly difficult matter to experimentally measure absolute reflectivities, the rotation diagrams *per se* do not seem to be particularly useful for obtaining geometrical information about the surface region. They may, however, be useful in some data-averaging scheme for obtaining structural information.[20–22]

IV. SUMMARY

In this paper we used a version of the inelastic collision model incorporating three partial wave components to calculate LEED rotation diagrams for Al(100). These calculated rotation diagrams were compared with existing experimental data with mixed results. For an energy of 50 eV and an incident angle of 32° the agreement between theory and experiment was satisfactory, but this was not the case for an energy of 20 eV and an incident angle of 50°. This is not too surprising in view of the highly simplified model for the electron-solid force law that was used in the theoret-

ical calculations. This model neglected the details of the interaction of the electron with the induced surface charge and also neglected, specifically, surface effects such as the surface-plasmon contribution to the electronic self-energy.[23-25] These effects will become increasingly important for large angles of incidence—especially for low electron energies. The theoretical model also did not include the effects of the surface-state resonances.[2-5] However, the model calculations did produce a broad resonancelike structure in the (00) beam at $E = 20$ eV and $\theta = 50°$ at a place where structure attributed to a surface-state resonance occurs in the experimental data. Our calculation did not provide a satisfactory description of this resonance structure, but thus far, neither have model calculations,[19] which include the effects of a surface potential. The effect of small changes in the upper-layer spacing on the calculated rotation diagrams was also investigated. The primary change that occurred was in the over-all beam intensities and not in the qualitative shape of the rotation diagrams. Thus, it is felt that rotation diagrams *per sec* are not especially useful for obtaining geometrical information about the surface region. They may, however, be useful in various data-averaging schemes for analyzing experimental data.[20-22] In closing, we note that the apparent insensitivity of the rotation diagrams to small changes in the surface geometrical parameters may be an asset in using the rotation diagrams to look at various resonance effects.

ACKNOWLEDGMENT

I would like to thank D. G. Schreiner for his assistance in plotting the experimental curves.

---

*Work supported by the U. S. Atomic Energy Commission.

[1]In the kinematic limit a LEED energy profile would consist of a series of primary Bragg peaks. Multiple scattering effects split these primary Bragg peaks into multiple scattering clusters which are located near the kinematical Bragg position. See, for example, C. W. Tucker, Jr. and C. B. Duke, Surface Sci. 24, 31 (1971).

[2]E. G. McRae, J. Chem. Phys. 45, 3258 (1966).

[3]K. Hirabayashi, J. Phys. Soc. Japan 25, 856 (1968).

[4]E. G. McRae, Surface Sci. 25, 491 (1971).

[5]P. J. Jennings, Surface Sci. 25, 513 (1971).

[6]J. Lauzier, L. de Bersuder, and V. Hoffstein, Phys. Rev. Letters 27, 735 (1971).

[7]L. de Bersuder, V. Hoffstein, and J. Lauzier, Surface Sci. 27, 338 (1971).

[8]R. Baudoing, L. de Bersuder, C. Gaubert, V. Hoffstein, J. Lauzier, and H. Taub, J. Vac. Sci. Technol. 9, 634 (1972).

[9]G. E. Laramore and C. B. Duke, Phys. Rev. B 5, 267 (1972).

[10]G. E. Laramore, C. B. Duke, A. Bagchi, and A. B. Kunz, Phys. Rev. B 4, 2058 (1971).

[11]F. Jona, IBM J. Res. Develop. 14, 444 (1970).

[12]In this paper we follow the notation of Refs. 6–8 and label the beams according to the nonprimitive cubic two-dimensional cell.

[13]C. B. Duke and C. W. Tucker, Jr., Phys. Rev. Letters 23, 1163 (1969).

[14]D. T. Quinto and W. D. Robertson, International Conference on Solid Surfaces (unpublished); D. T. Quinto, B. W. Holland, and W. D. Robertson, Surface Sci. 32, 139 (1972).

[15]G. E. Laramore, Phys. Rev. B 6, 1097 (1972).

[16]E. C. Snow, Phys. Rev. 158, 683 (1967).

[17]C. B. Duke and G. E. Laramore, Phys. Rev. B 2, 4765 (1970).

[18]G. E. Laramore and C. B. Duke, Phys. Rev. B 2, 4783 (1970).

[19]H. Taub, Surface Sci. 30, 161 (1972).

[20]M. G. Lagally, T. C. Ngoc, and M. B. Webb, Phys. Rev. Letters 26, 1557 (1971).

[21]M. B. Webb and M. G. Lagally, Proceedings of the Fifth Low-Energy-Electron-Diffraction Seminar, 1971 (unpublished).

[22]C. B. Duke and D. L. Smith, Phys. Rev. B 5, 4730 (1972).

[23]C. B. Duke and G. E. Laramore, Phys. Rev. B 3, 3183 (1971).

[24]G. E. Laramore and C. B. Duke, Phys. Rev. B 3, 3198 (1971).

[25]P. J. Feibelman, C. B. Duke, and A. Bagchi, Phys. Rev. B 5, 2436 (1972).